Resources, Conservation & Recycling 222 (2025) 108439

Contents lists available at ScienceDirect

Resources, Conservation & Recycling

journal homepage: www.sciencedirect.com/journal/resources-conservation-and-recycling

Full length article

Re-directing mixed-feed deconstruction products to hybrid polyesters: Tolerance windows for commodity plastics reconstruction

Ryan W. Clarke [a,b], Briona J. Carswell [c], Jason S. DesVeaux [b,d], Levi J. Hamernik [a,b], Clarissa Lincoln [a,b], Vinod K. Konaganti [e], Rufina G. Alamo [c], Katrina M. Knauer [a,b,*]

[a] Renewable Resources and Enabling Sciences Center, National Renewable Energy Laboratory, Golden CO 80401, USA
[b] BOTTLE Consortium, Golden, CO 80401, USA
[c] Florida A & M and Florida State University, College of Engineering, Tallahassee, FL 32310, USA
[d] Catalytic Carbon Transformation and Scale-Up Center, National Renewable Energy Laboratory, Golden, CO 80401, USA
[e] Amazon Corporation, Seattle, WA 98109, USA

ARTICLE INFO

Keywords:
Chemical recycling
Plastics
Polyesters
Monomer separations
Polycondensation

ABSTRACT

Solvolysis is a promising strategy for mixed-feed polyester recycling, but little attention has been given to downstream product separations or the impact of using imperfectly separated monomer mixtures in recycled polymer reconstruction. Here, we challenge the traditional need for high-purity monomers in polycondensation synthesis of engineering thermoplastics. Monomer mixtures are derived from catalyzed methanolysis of polyethylene terephthalate (PET), polybutylene terephthalate (PBT), and polybutylene adipate-*co*-terephthalate (PBAT), with separation scenarios ranging from high (99:1) to low (90:10) purity. We focus on challenging-to-separate products like ethylene glycol and 1,4-butanediol and evaluate tolerance for comonomer incorporation in recycled hybrid polyesters: polybutylene-*co*-ethylene terephthalate (PBET) and polybutylene ethylene adipate-*co*-terephthalate (PBEAT). Evaluations are made between "contaminant" monomer incorporation, and the resulting materials' thermal properties, crystalline structure, tensile toughness, and rheology. Ultimately, we highlight that despite incorporation of contaminant monomer, high-performance hybrid polyesters of PET, PBT, and PBAT are obtained while reducing the strain of high-throughput separations.

1. Introduction

Calls for modernization of the global material economy have motivated a shift from the current linear flow (production, use, discard) to a circular flow (production, use, recycle) of polymers. (Nixon et al., 2024; Vidal et al., 2024; Coates and Getzler, 2020) The development of high-performance, designer polyester materials has emerged as one of the most compelling strategies for renewable and recyclable alternatives to incumbent thermoplastics. Specifically, the backbone ester linkage is a convenient functional group enabling numerous recycling chemistries such as deconstruction or depolymerization to monomer. (Shi et al., 2024; Clark and Shaver, 2024; Schwab et al., 2024; Cao et al., 2024; Weng et al., 2023; Cao et al., 2022; Hong and Chen, 2017; Xu and Wang, 2022) Advancements have been made to improve the sortation of similar polymers (like polyesters) through the implementation of infrared-based identification and artificial intelligence (AI) tools. However, a materials economy dominated by polyester materials are less prone to the limitations of preliminary sorting in plastics recycling, as such a system could conceivably be managed at end-of-life by a single, compatible deconstruction strategy.

Polyester materials are already ubiquitous in modern technologies. Aromatic polyesters polyethylene terephthalate (PET) and polybutylene terephthalate (PBT) currently comprise a significant fraction of annual polymer manufacture, (Nicholson et al., 2021) while compostable polylactic acid (PLA) and polybutylene terephthalate-*co*-adipate (PBAT) are garnering increased attention and marketspace as sustainable plastic alternatives. (Biodegradable Plastics Market Global Forecast to 2029, 2024) In many of these systems, chemical depolymerization returns monomer products readily capable of direct repolymerization following separation and purification (Fig. 1A). Specifically, catalyzed solvolysis techniques such as hydrolysis, alcoholysis, and glycolysis have been applied to PET, (Aguado et al., 2023; Barnard et al., 2021) PBT, (Loyer

* Corresponding author at: Renewable Resources and Enabling Sciences Center, National Renewable Energy Laboratory, BOTTLE Consortium, Golden, CO 80401, USA.
E-mail address: katrina.knauer@nrel.gov (K.M. Knauer).

https://doi.org/10.1016/j.resconrec.2025.108439
Received 7 March 2025; Received in revised form 29 May 2025; Accepted 1 June 2025
Available online 10 June 2025
0921-3449/© 2025 The Authors. Published by Elsevier B.V. This is an open access article under the CC BY license (http://creativecommons.org/licenses/by/4.0/).

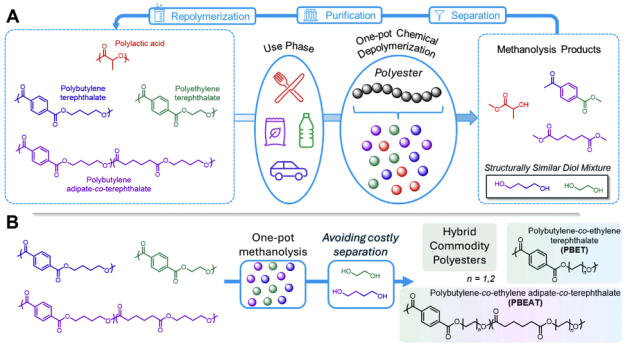

Fig. 1. Polyester Closed-Loop Recycling. (A) Current proposed pathway for mixed commercial polyester closed-loop life cycle under catalyzed methanolysis, separation, purification, and repolymerization process. **(B)** Generalized concept of this work toward relieving separation toll associated with diol mixtures and promoting downstream methanolysis harmony by evaluating hybridized analogues of PET, PBT, and PBAT.

et al., 2021; Jie et al., 2006) PLA, (Li et al., 2024) and PBAT, (Zheng et al., 2024; Pang et al., 2024; Shen et al., 2023) yielding the corresponding monomers which can be readily reconstructed by polycondensation. Mixed-feed systems have also been established utilizing a variety of polyester materials, supporting solvolysis as a universal method for managing complex end-of-life waste-streams and have been thoroughly reviewed. (Spicer et al., 2024; Andini et al., 2024; Arifuzzaman et al., 2023; Yang et al., 2022; Sardon et al., 2021; Yang et al., 2020) Despite this advantage, there has been little consideration for how the resulting mixed monomer products would be handled regarding efficient separations in a real-world scenario.

We recently analyzed and compared techno-economic analyses (TEAs) and life-cycle assessments (LCAs) for the methanolysis, hydrolysis, and glycolysis of mixed polyester feedstocks. (DesVeaux et al., 2024) Here we identified methanolysis as the most cost- and carbon-efficient pathway for mixed polyester feedstocks when compared to hydrolysis and glycolysis (Fig. 1A). (DesVeaux et al., 2024) Operating under this guidance with model substrates of PET, PBT, and PBAT, dimethyl terephthalate (DMT), dimethyl adipate (DMA), ethylene glycol (EG), and butanediol (BDO) monomer products are expected. In this scenario, while the separation of DMT and DMA can be achieved by simple filtration, the separation of the EG and BDO mixture by distillation is not so straightforward due to strong hydrogen-bonding and structural similarity (Fig. 1A). In line with typical separation principles, increasing purity of separated products comes at the expense of complexity, time, and energy. On the other hand, one could instead question if there is some threshold for how stringent separation and purification must be in order to obtain a useful, second-life material. For example, polycondensation between DMT and a 98:2 mixture of EG:BDO may be inconsequential for obtaining a PET-like polymer with marginally altered material properties, while dramatically reducing monomer purification costs.

To this end, we consider the impact of monomer "contamination" by evaluating the re-direction of PET, PBT, and PBAT methanolysis products to hybrid polyesters polybutylene-*co*-ethylene terephthalate (PBET) and polybutylene-*co*-ethylene adipate-*co*-terephthalate (PBEAT) by mixed-feed polycondensation (Fig. 1B, Fig. S1). A stand-alone TEA model was employed to assess the costs and benefits of downstream EG and BDO distillation in a methanolysis process and to identify optimal monomer ratios for reconstruction, aiming to minimize costs and energy demands in the separation design. Mixtures of EG:BDO are predesignated to emulate correspondingly low (90 mol %), medium (95 mol %), and high (99 mol %) monomer purity. Each mixture containing the "contaminant" monomer (EG for PBAT, BDO for PET) is employed in polycondensation alongside DMT for PBET, as well as DMT and DMA for PBEAT. Spectroscopic analysis by nuclear magnetic resonance spectroscopy (NMR) reveals an important bias toward increased BDO loading in the final polyester due to the release of more volatile EG during chain-growth. Trends in contaminant loading deviation are moderately correlated between the three ratios, suggesting that final product composition can be reliably targeted. Compared to commercial polyester controls, hybrid polyesters have substantially high molar mass (HMM) (up to nearly 100 kg mol^{-1}) and 2–10× higher zero-shear viscosity. Hybrid polyesters also exhibit good mechanical properties by tensile strength (~30 MPa PBET, ~25 MPa PBEAT), tensile strain (~150 % PBET, ~600 % PBEAT), and Young's modulus (~3 GPa PBET, ~0.1 GPa PBEAT). Small-angle and wide-angle X-ray scattering insights (SAXS and WAXS, respectively) show that monomer contamination does impact long range order and crystallinity in hybrid polyesters which may affect processing conditions downstream. However, inclusion of hybrid polyesters (~5 wt. %) when compounding PET and PBAT, respectively, show little effect on overall PET and PBAT properties. Overall, we demonstrate that valuable materials can be prepared with slightly altered comonomer composition and retain candidacy for continuous methanolysis (and other solvolysis methods) and closed-loop recycling.

2. Results & discussion

2.1. Energy and economic incentives for mixed-monomer hybrid polyesters

We first conducted TEA to evaluate the energy requirements and installed equipment costs for distilling a mixture of EG and BDO. Aspen Plus V14 was used to simulate a distillation column (Fig. 2A, Tables S1-S2) for the purification of 2000 kg h^{-1} of a feed mixture of 90/10 % EG and BDO and 90/10 % BDO and EG, respectively. These cases were selected to represent PET-rich (current) and PBAT-rich (hypothetical future) scenarios. The mixtures were distilled across a range of product purities from 90 % to 99.95 % to highlight the increasing energy demand and equipment cost that result from more stringent purification (Fig. 2B-C). For example, the energy required to distill an incoming mixture of 90/10 % EG/BDO approximately triples from a purity of 97.5 % to >99 %, whereas the energy for a 90/10 % BDO/EG mixture quadruples (Fig. 2B, Table S1). The direct installed equipment cost for the column also increases with purity primarily due to the requirement for larger column condensers and reboilers (Fig. 2C, Table S2). A more dramatic change in equipment cost is observed for the EG case due to EG being the more volatile (lower boiling point than BDO) species that is stripped from the mixture therefore requiring a larger, more expensive column at high concentrations. These results highlight the energy consumption and capital expenses if comonomer purity requirements can be reduced for polycondensation synthesis.

2.2. Implications of mixed-monomer streams for hybrid polyester reconstruction

Hybrid polyesters were compared against commercially available PET (bottle grade, 25.7 kg mol^{-1}), PBT (extrusion grade, 26.9 kg mol^{-1}), and PBAT (film grade, 26.3 kg mol^{-1}, ~50:50 mol % DMT:DMA) (Figs. S2-S4). Hybrid polycondensation mixtures considered downstream scenarios in which separation of DMT and DMA have been performed, leaving the EG and BDO mixture. Ratios of 99:1, 95:5, and 90:10 (mol ratio) diol mixtures were selected to reflect simulated separation intensity ranging high-, medium-, and low-throughput, respectively (Fig. 1A). Furthermore, identification by PBET-1, −2, and 3 or PBEAT-1, −2, and −3 correspond to initial loadings of 99:1, 95:5, and 90:10 mol % EG:BDO (PBET) and BDO:EG (PBEAT) (Table S3) (Fig. 3).

From gel permeation chromatography (GPC), PBET-1, −2, and −3, exhibited number-averaged MM values (M_n) ranging 98.7 kg mol^{-1}, 78.6 kg mol^{-1}, and 57.6 kg mol^{-1}, respectively (Figs. S5-S7). The trend in reduced MM with increase in BDO loading is accredited to the higher

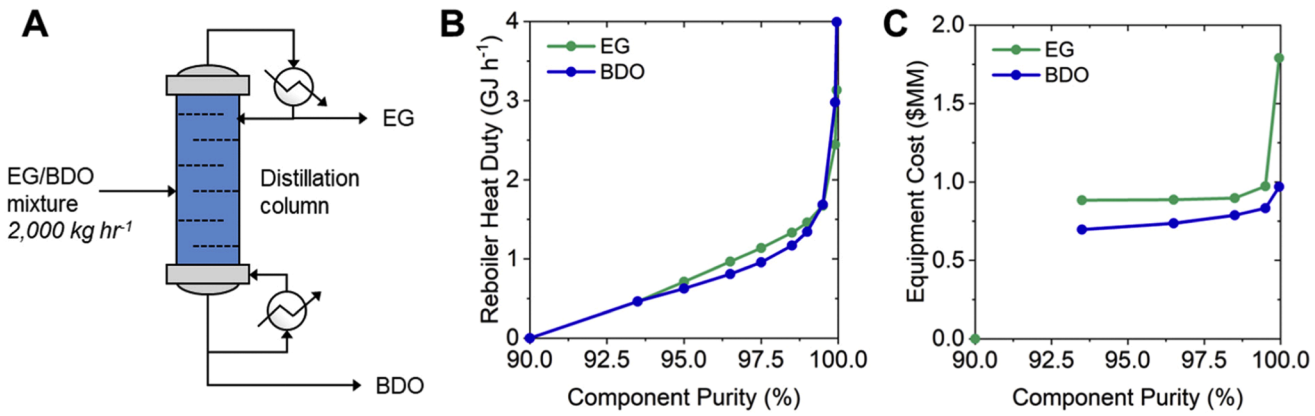

Fig. 2. TEA for EG/BDO Separation. A) Diagram for the distillation of a mixture containing 2000 kg/h of EG and BDO resulting in a purified EG distillate and BDO bottoms product. **B)** Required reboiler duty in GJ h^{-1} for the distillation of a starting 90/10 wt. % mixture of EG/BDO (EG case in plot) and a 90/10 wt. % mixture of BDO/EG (BDO case in plot) following chemical depolymerization across a range of product purity in wt. % and **C)** the associated direct installed equipment cost in millions of dollars ($MM) for the distillation column. Component purity refers to the distillate EG product for the EG case and the BDO bottoms product for the BDO case.

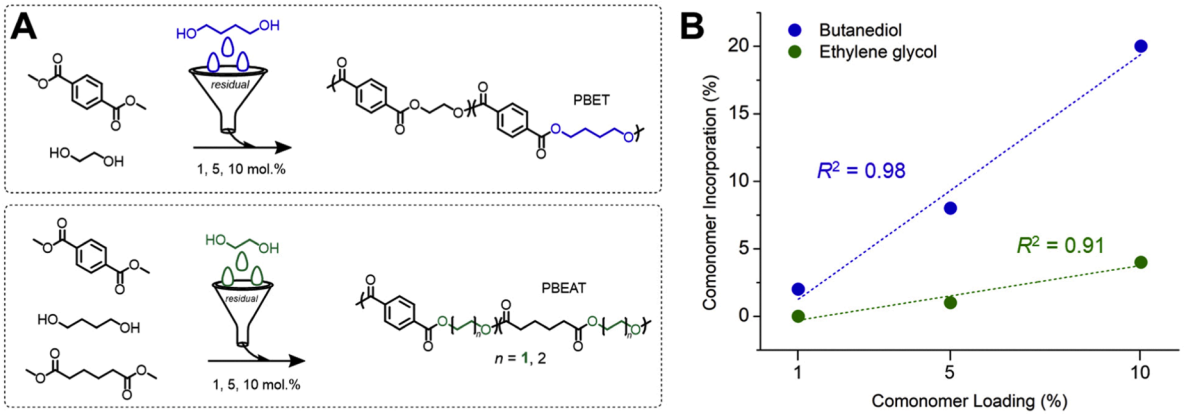

Fig. 3. Hybrid Polyester Synthesis and Incorporation Bias. A) General scheme for the polycondensation of DMT, DMA, EG, and BDO as specified toward hybrid PBET and PBEAT (180 °C for 16 h under N_2, 240 °C for 2 h under N_2, 280 °C for 6 h under 2 Torr). **B)** Discrepancy between contaminant EG (green) and BDO (blue) loadings in PBEAT and PBET, respectively, and observed polymer incorporation.

boiling point (BP) of BDO, which hinders diol removal during late-stage condensation step-growth. On the other hand, PBEAT-1, −2, and −3 had a moderately lower range of M_n values of 39.7 kg mol^{-1}, 77.9 kg mol^{-1}, and 31.8 kg mol^{-1}, respectively (Figs. S8–10). Nonetheless, each of the hybrid polyesters have similar or higher MM to the commercial analogues while at suitably HMM for critical chain entanglement and, thus, proper thermomechanical behaviors. Worth noting, all synthesized hybrid polyesters were obtained as white fibrous precipitates, indicating high purity (Fig. S11)

2.3. Structural characterization of hybrid polyesters

We first conducted structural characterization of all 6 hybrid polyesters to observe deviations between initial loading and final comonomer incorporation (Table S3). Considering the difference in BP between the two diols, we surmised there would be a discrepancy between the initial loading and the final hybrid polyester diol composition. As BDO has a higher BP than EG, we anticipated a bias in which BDO composition would be higher than initially targeted, while EG composition would be lower than initially targeted. Such implications would be highly beneficial for obtaining PBAT-like materials despite the presence of EG contaminant as a form of reactive purification, but potentially challenging for obtaining PET-like materials with minor contamination of BDO. In agreement, ^{1}H NMR of PBET hybrids 1 (1 % loading), 2 (5 % loading), and 3 (10 % loading) exhibited final BDO content of 2 %, 8 %, and 20 %, respectively (Fig. 1B, Fig. S12). Additionally, PBEAT hybrids 1 (1 % loading), 2 (5 % loading), and 3 (10 % loading) displayed final EG incorporation of 0 %, 1 %, and 2 %, respectively (Fig. S13). The results here demonstrate a reasonable expectation that preliminary BDO contamination in PET synthesis feedstock will propagate to nearly 2× incorporation in the final product, while EG contamination in PBAT feedstock will return at least 5× less final incorporation, pending reaction time and polymer MM.

We also employed ^{13}C NMR to elucidate hybrid polyester structures, which may be present as blocky or random (statistical) (Figs. S14-S15). We anticipated this could be visualized by the presence of intermediate carbonyl peaks between the characteristic signals of PET and PBT, representing junction units, or matching carbonyl peaks signaling homopolymer blocks. In the case of PBET, we observed that low incorporation of BDO comonomer (PBET1, 2 %; PBET2, 8 %) returned trace signals of the junction peaks supporting statistical copolymer architectures (Fig. 4A). On the other hand, higher BDO incorporation (PBET3, 20 %) returned both junction peaks between PET and PBT units as well as signals corresponding to PBT homopolymers, highlighting a mixture of PET-PBT statistical and block copolymer architectures (Fig. 4A). Unsurprisingly, hybrid PBEAT materials with low EG incorporation (PBEAT-2, −3, 1–2 %) did not show any change in carbonyl signal, supporting the inconsequential effect of up to 10 % contaminant

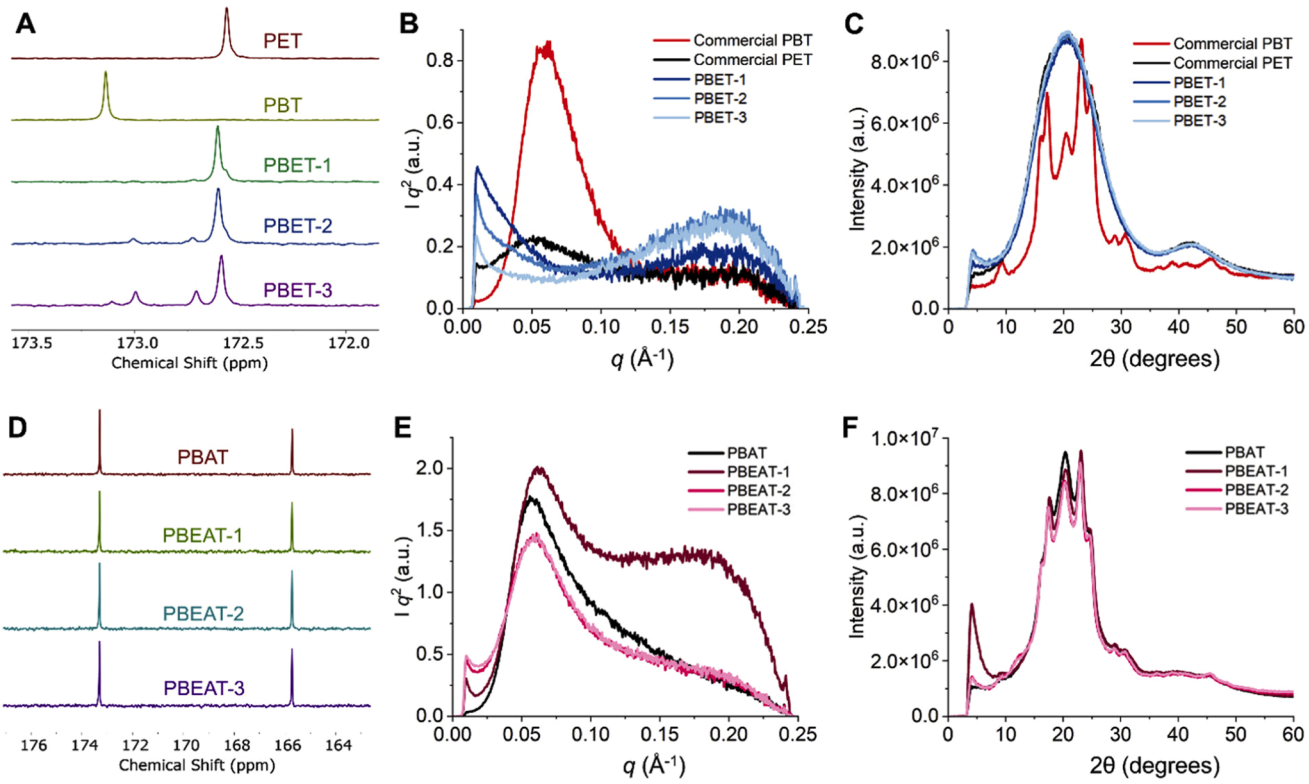

Fig. 4. Structural Analysis of Hybrid Polyesters. A) ^{13}C NMR (TFA+$CDCl_3$) analysis of PET, PBT, and PBETs 1–3 architectures highlighting the carbonyl region. **B)** SAXS and **C)** WAXS profiles for PET, PBT, and PBETs 1–3. **D)** ^{13}C NMR ($CDCl_3$) analysis of PBAT and PBEATs 1–3 architectures highlighting the carbonyl region. **E)** SAXS and **F)** WAXS profiles for PBAT and PBEATs 1–3.

monomer (EG) feed during polycondensation for PBAT materials (Fig. 4D).

WAXS and SAXS measurements were conducted on the synthesized polyesters to show the impact of monomer impurity on the crystalline structures and long-range order of the polymers when compared to their commercial counterparts. Figs. 4B and C reveal how randomly interspersed units of BDO (2 – 20 %) affect chain packing and long-range periodicity of PBET hybrids. Under the same processing conditions from the melt, sharp diffraction reflections consistent with the triclinic lattice of crystalline PBT are only observed in commercial PBT (51 % crystallinity based on WAXS profile, **Fig. S16**). (Mencik, 1975) As shown, PET and hybrid PBET are largely amorphous, and the SAXS patterns reflect these features as well (Fig. 4B). The sharp intense SAXS scattering peak is characteristic of a semicrystalline structure with a relatively high linear crystallinity for the PBT specimen. The long-period or distance between lamellar crystallites of PBT is 107 Å, and the shallow low-intensity SAXS peak of PET indicates the presence of a small content of imperfect aggregates with long-range periodicity of ~114 Å. Conversely, the random incorporation of up to 20 % BDO in PET, suppresses crystallinity on quenching from the melt state, resulting in amorphous PBET hybrids with no WAXS reflections and no scattering SAXS peaks.

The SAXS and WAXS profiles of PBAT and corresponding hybrid PBEAT random copolymers are given in Figs. 4E and F, respectively. It was concluded that PBAT copolymers with < 20 mol % BT units crystallize in the PBA monoclinic lattice, (Cranston et al., 2003; Gana et al., 2003; Minke and Blackwell, 1979) while copolymers with >30 mol % BT units crystallize in the triclinic BT lattice. The WAXS patterns of PBAT and PBEAT hybrids (Fig. 4F) are consistent with the monoclinic phase of PBA and follow the isomorphic PBA structure expected from prior work. The levels of crystallinity of PBAT and PBEAT hybrids obtained from the WAXS patterns are 37 ± 3 % indicating that EG units, when incorporated into the chain up to 2 %, exert a negligible effect on the semicrystalline structure of PBEAT hybrids. The same conclusion is reached from the SAXS patterns (Fig. 4E) which correspond to long periods of 105 ± 2 Å for all.

2.4. Thermal properties of hybrid polyesters

As PET and PBT often rely on their levels of crystallinity for various performance advantages, we next probed the implications of comonomer incorporation on hybrid polyesters' chain-packing and semicrystalline structure on their corresponding thermal behaviors. Thermal properties on the first heating scan are reflective of the polymer performance in adjacent analyses and are thus most important. Under compression molding, films of commercial PBT and PBAT are semicrystalline, while PET is almost entirely amorphous as indicated by the X-ray patterns and a cold crystallization event at 125 °C (Fig. 5A). The DSC (first melting) glass transition temperatures (T_g) of PET, PBT, and PBAT are 70 °C, 47 °C, and −28 °C, and the melt transition temperatures (T_m) are 245 °C, 221 °C, and 121 °C, respectively (Fig. 5A,D, Table S4). The endothermic transition at 50 °C observed in the first scan of PBAT is associated with formation of small and defective crystallites in the interlamellar regions of the initially formed crystals. These defective crystallites are formed during aging at room temperature and have been observed in other semicrystalline random copolymers. (Alizadeh et al., 1999)

Conceivably, as PBET hybrids transition from BDO-trace (PBET-1) to BDO-rich (PBET-3), we anticipate some magnitude of crystallinity disruption observable by T_m and enthalpy of fusion (ΔH_f). Indeed, PBET-1, −2, and −3 samples exhibited decreased T_m (to PET, 245 °C) of 240 °C, 232 °C, and 218 °C with diminishing ΔH_f (to PET, 46.3 J g^{-1}) of 38.3 g^{-1}, 36.7 J g^{-1}, and 34.2 J g^{-1}, paralleling increased BDO incorporation (Fig. 5A, Table S4). A clear trend is also observed in the second heating scan and the cooling scan, where higher BDO loading again returns a decreasing T_m and crystallization temperature (T_c) with increasing BDO

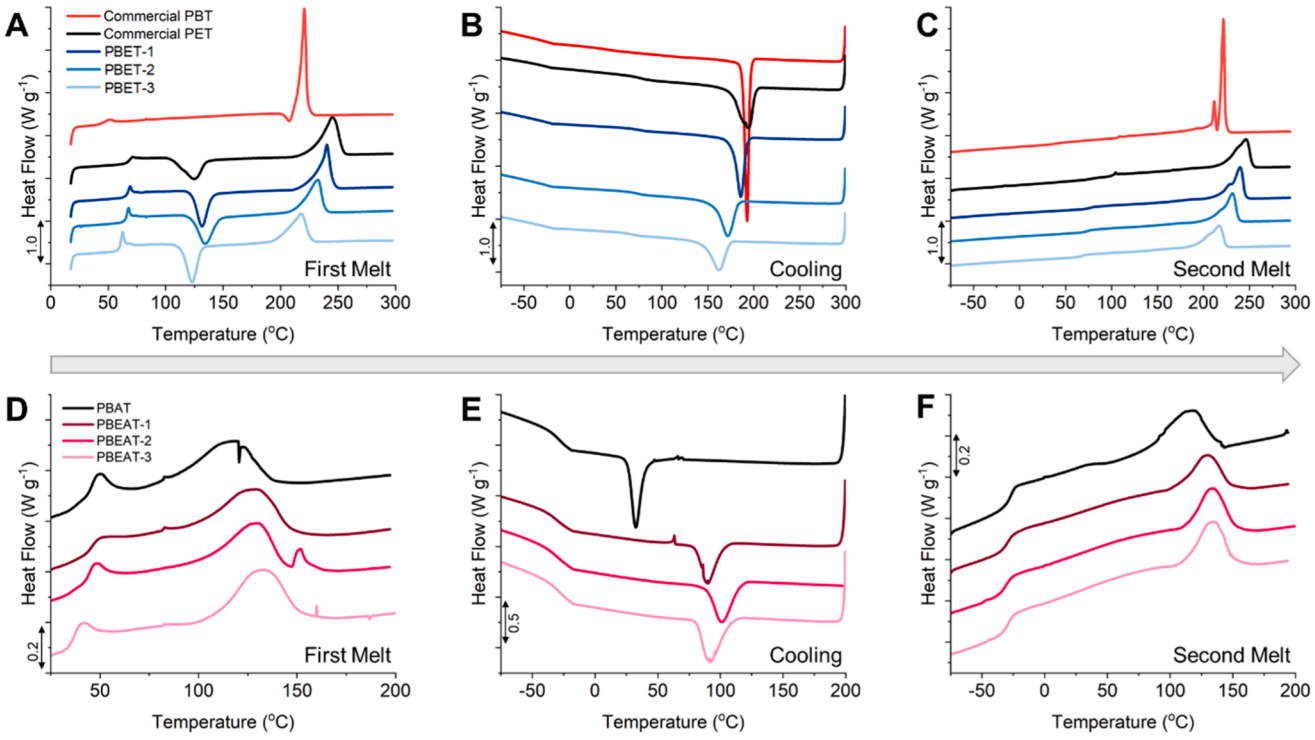

Fig. 5. Evolution in Hybrid Polyester Thermal Properties with Comonomer Loading. DSC traces (exo-down) encompassing **A)** heating scan 1 (25 °C to 300 °C, 20 °C min^{-1}), **B)** cooling scan 1 (300 °C to −80 °C, 20 °C min^{-1}), and **C)** heating scan 2 (−80 °C to 300 °C, 20 °C min^{-1}) for PET, PBT, and PBETs 1–3 (blues). **D)-F)** Similar DSC traces for PBEAT 1–3 (pinks) alongside commercial (black) (25 °C to 200 °C to −80 °C to 200 °C, 20 °C min^{-1}).

incorporation (Fig. 5B-C, Table S3). Aside from crystalline properties, we also observe decreasing T_g in PBET-1, −2, and −3 (68 °C, 66 °C, and 62 °C) (Fig. 5A).

On the other hand, we observed that PBEAT-1, −2, and −3 returned increasing T_m all of which the major crystalline domain melts at 129 °C with varying degrees of ΔH_f (to 29.8 J g^{-1} for PBAT) ranging 20.2 – 32.4 J g^{-1} (Fig. 5D). Crystals formed on aging melt near 48–49 °C, and additional minor melt peaks are observed at 151–154 °C on the first scan (Table S4), though absent in the second heating scan, thus suggesting the latter is an artifact of film processing conditions (Fig. 5F). Similarly, T_c values in all PBEAT samples also exhibit significant increase (+65 – 75 °C) compared to PBAT (32.4 °C) (Fig. 5E). Notably, there was no change in the PBEAT T_g (−28 °C) compared to commercial PBAT (−28 °C). Considering that PBEAT-1 has similar MM but no observable incorporation of EG, we surmise the higher T_m and T_c may reflect plasticizers and additives present in the commercial PBAT sample. Ultimately, increasing contaminant monomer composition has a direct effect on hybrid polyester crystallinity and T_m, though high melt stability is retained at these moderate loadings.

2.5. Mechanical and rheological properties of hybrid polyesters

We next evaluated the mechanical properties of the hybrid polyesters by tensile testing to determine consequences of introducing contaminant diol monomer incorporation. Specifically, we monitored the evolution in stress at break (σ_B), strain at break (ε_B), and Young's modulus (E) with different diol compositions by tensile testing (~23 °C, 5 mm min^{-1}) (Table S5). Though structurally similar aromatic polyesters, the adipic group in PBAT yields a significantly softer (σ_B = 41.8 MPa) and more ductile (ε_B = 1133 %) material than PET (σ_B = 54.5 MPa, ε_B = 306 %) and PBT (σ_B = 60.1 MPa, ε_B = 310 %) (Fig. S17-S18). The BDO linker in PBT also affords increased compliance or decreased stiffness (E = 1570 MPa) than PET (E = 1910 MPa), similarly reflected in a decreased yield strength (Fig. 7A). As hybrids, PBET 1 – 3 materials exhibited high ε_B 112 % – 143 %, though did not exhibit the same strain hardening effect as the commercial PET and thus also limited to a lower range of σ_B between 32.0 MPa – 36.5 MPa (Fig. 7A). Nonetheless, PBET-1, −2, and −3 each retained high yield strength measuring 53.1 MPa, 50.0 MPa, and 53.7 MPa and increased E between 1955 MPa - 2615 MPa (Table S5).

Similar conclusions are made for PBEAT-1, −2, and −3, where each sample demonstrated a tight range of ε_B and σ_B between 522 % – 587 % and 23.8 MPa – 28.9 MPa, respectively (Fig. 7B). Compared to the commercial PBAT, each PBEAT displayed marginally increased yield strength (10 MPa vs. 8.3 MPa) and E (98.3 MPa – 117 MPa) (Fig. S18, Table S5). The commercial sample displayed significantly higher tensile toughness by ε_B of 1158 % and strain hardening up to σ_B of 41.7 MPa. Furthermore, despite the respectively lower or similar MM between PET, PBT and PBAT to the corresponding hybrid polymers, commercial samples are significantly stronger and more ductile. Specifically, the PBEAT-1 (0 % EG incorporation) demonstrates an approximate 50 % reduction in ductility compared to the commercial analogue. We can seemingly only accredit these distinctions to either catalyst residue in the in-house synthesized polymers, or the presence of plasticizers or modifiers in the commercial controls. Regardless, both PBET and PBEAT have high-performance qualities despite contaminant comonomer incorporation by tensile testing which supports their ability to serve in similar applications.

Melt flow rheology was employed to evaluate translatability of PBET and PBEAT to commercial processing methods. As the polymer melt viscosity is a major governing factor for techniques such as blow molding and blown-film extrusion, we conducted flow experiments to monitor viscosity and shear-thinning response with varied shear rate (Table S7). Zero-shear viscosity (η_0), recorded as the initial near-zero shear rate (0.001 s^{-1}) plateau, was notably higher for PBET-1 (532 × 10 (Coates and Getzler, 2020) cP), PBET-2 (1287 × 10 (Coates and Getzler, 2020) cP), and PBET-3 (524 × 10 (Coates and Getzler, 2020) cP) than both PET (285 × 10 (Coates and Getzler, 2020) cP) and PBT (149 × 10 (Coates and Getzler, 2020) cP) (Fig. 6C). Clearly the hybrid polyester MM has a significant effect on this property, where both PBET-1 (98.7 kg mol^{-1}) and PBET-2 (78.6 kg mol^{-1}) have nearly double the η_0 of PET

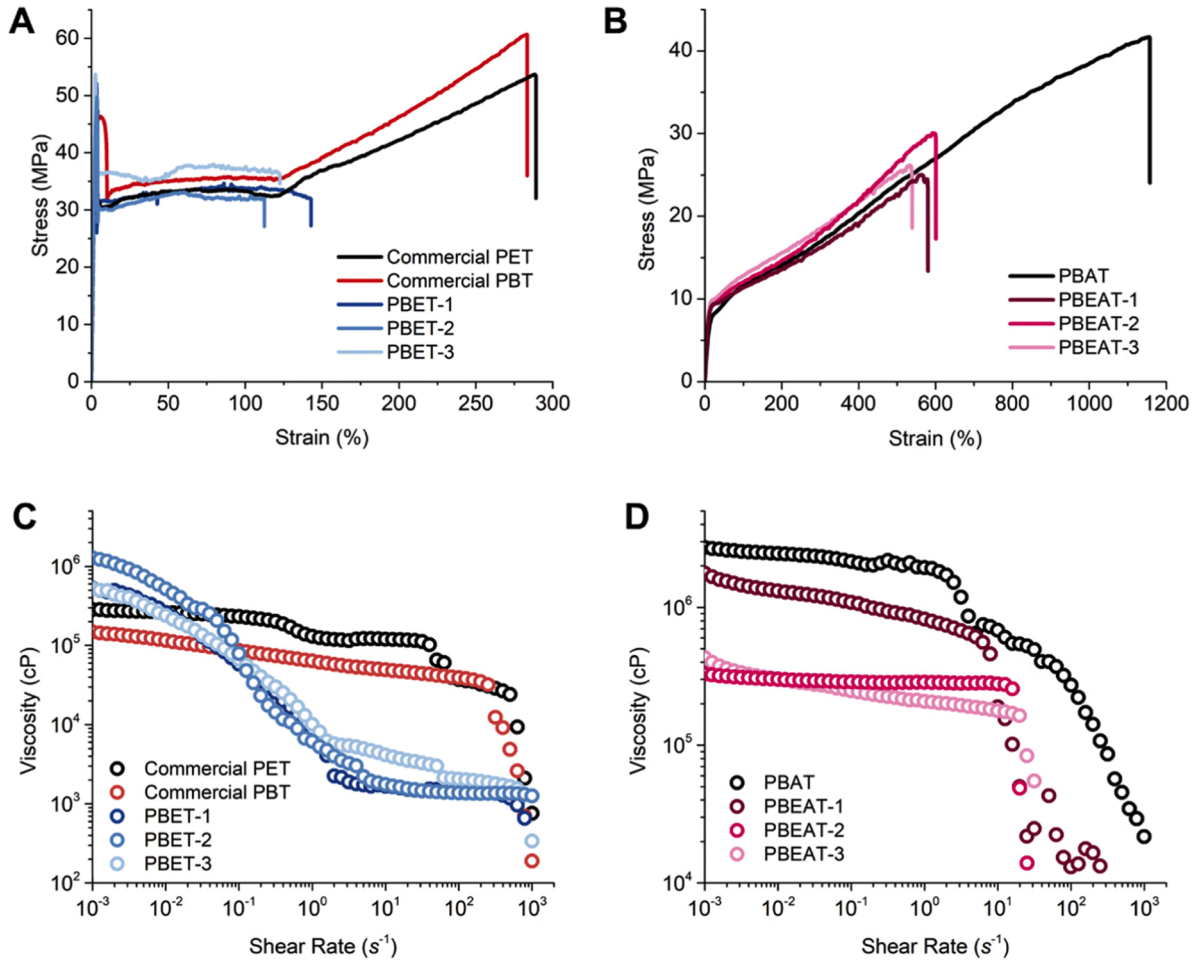

Fig. 6. Evolution in Hybrid Polyester Mechanical and Rheological Properties. Representative tensile stress/strain (ASTM D638–5, ~23 °C, 5 mm min^{-1}) curves for **A)** PBET-1, −2, and −3 (blues) alongside commercial PET (black) and PBT (red), as well as for **B)** PBEAT-1, −2, and −3 (pinks) alongside commercial PBAT (black). **C)** Rheological flow curves for PBET-1, −2, and −3 (blues) alongside commercial PET (black) and PBT (red) (280 °C), as well as for **D)** PBEAT-1, −2, and −3 (pinks) alongside commercial PBAT (black) (175 °C).

and PBET-3 (57.6 kg mol^{-1}) (Figs. S19-S20). Also worth noting, we observed a consistent earlier onset of shear thinning with each PBET material (~0.1 s^{-1}) compared to pure PET or PBT (~500 s^{-1}). This may be due to employing the same temperature (280 °C) despite the PBET hybrids having lower T_m values. Conversely, PBEAT-2 and PBEAT-3 exhibited nearly 3× lower η_0 (329 × 10 (Coates and Getzler, 2020) cP and 432 × 10 (Coates and Getzler, 2020) cP, respectively) than PBAT (2776 × 10 (Coates and Getzler, 2020) cP) but very similar points of shear thinning onset (~1 s^{-1}) (Fig. 6D). This drop may be due to lower EG comonomer contamination, as the PBEAT-1 sample with undetectable EG incorporation had a much higher viscosity of 1771 × 10 (Coates and Getzler, 2020) cP.

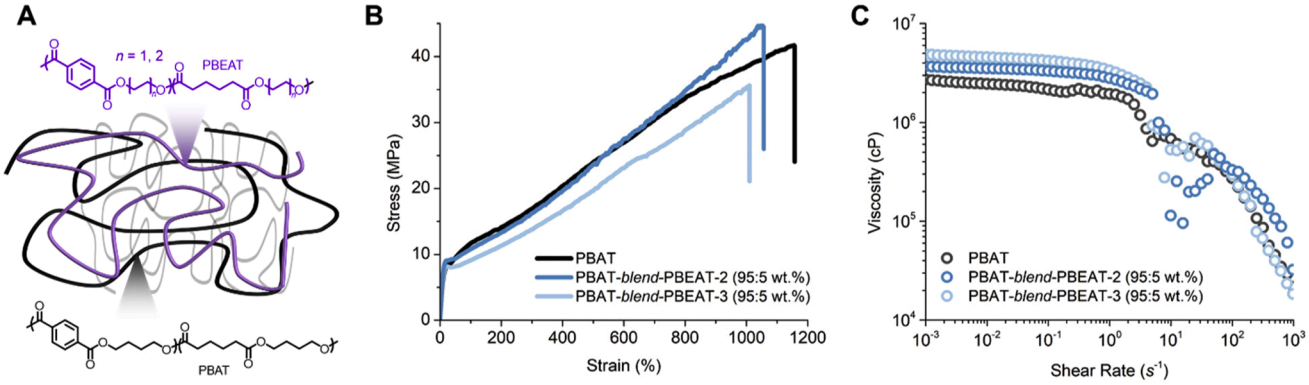

Fig. 7. Batch PBAT Performance with PBEAT Influx. A) Illustrated physical blending (master batching) of 5 wt. % PBEAT in majority composition (95 wt. %) PBAT, assuming high miscibility. **B)** Tensile stress/strain (~23 °C, 5 mm min^{-1}) curves for 95:5 blends of PBAT (black) with PBEAT-2 and −3 (blues), respectively. **C)** Flow rheology curves highlighting viscosity as a function of shear rate for 95:5 blends of PBAT (black) with PBEAT-2 and −3, respectively (175 °C).

2.6. Evaluating hybrid polyester implications for large batch manufacturing

Considering that the new polymers have deviated flow profiles in comparison to the commercial samples, we questioned how this could affect commercial PET and PBAT properties if PBET and PBEAT were a minor fraction of a compounded batch (Fig. 7A). To do so, we selected PBEAT to be considered as polymer contamination in a 95:5 blend ratio (95 wt. % PBAT, 5 wt. % PBEAT). In this case, tensile testing revealed significantly higher elongation at break of 1057 % and 1010 % despite blending in 5 wt. % of PBEAT-2 and PBEAT-3, respectively (Fig. S21). Even more interesting was the increase in σ_B from 41.7 MPa (PBAT) to 44.8 (PBEAT-3), which is likely due to the addition of HMM polymer (98.7 kg mol^{-1}) for enhanced entanglements (Fig. 7B). Similarly, we received much more consistent flow curves by melt flow rheology, with all shear-thinning onset occurring at ~5 rad s^{-1} (Figs. S22). The η_0 was also enhanced above that of pure PBAT to 3689 × 10 (Coates and Getzler, 2020) cP (PBAT-*blend*-PBEAT-2) and 4878 × 10 (Coates and Getzler, 2020) cP (PBAT-*blend*-PBEAT-3) (Fig. 7C). Worth mentioning, scanning electron microscopy of the blend cross-sections showed no significant sign of phase separation or micro-domain formation, indicating a high degree of mixing (Figs. S23-S24). These results indicate that if polyesters are reconstructed from low-throughput deconstruction products separation in one batch and compounded with traditional commodity polyesters in a separate batch, the cumulative batch will not suffer critical property changes.

3. Conclusion

In summary, this work aims to begin questioning depolymerization down-stream strategies considering calls for a circular, all-polyester material economy and corresponding chemical recyclability. Though polyester depolymerization can be conducted in mixed-feed, consideration must be made for how complex waste streams can be efficiently separated, or in this case, consolidated to make new materials that retain candidacy for re-entering that same depolymerization process. In this work, we highlight the substantial challenge of EG and BDO mixture separation, inevitable to surface in polyester recycling, and propose a solution of mixed-monomer feedstocks for reconstruction of hybrid polyesters PBET and PBEAT. We utilize polycondensation techniques to construct these hybrids with HMM structures between 39.7 kg mol^{-1} – 98.7 kg mol^{-1}, while dosing in contaminant EG (to PBAT) or BDO (to PET) comonomers in 1, 5, and 10 mol. % loadings. By NMR, we observe that pre-designated comonomer loading is offset to yield roughly 2–5× higher loadings of BDO in the final PBET polymer, and conversely roughly 1–3× lower loadings of EG in the final PBEAT polymer, as a result of differences in comonomer volatilities. Valuable properties such as levels of crystallinity, high tensile toughness, and shear thinning by melt processing are retained in lieu of comonomer embedment, though more work could be done to understand the impact on permeation or barrier properties for using PBET and PBEAT in packaging applications. Lastly, we demonstrate inconsequential effects of compounding minor compositions of PBEAT into industrial batches of PBAT, which rectifies any hybrid deviations in performance when in bulk. It is important to note that other contaminants identified in post-consumer polyester waste streams such as dyes and additives were not considered in this evaluation. While dyes and metals can be removed via activated carbon treatment or ion exchange membrane filtration, additives can linger in distillation products. These small molecules can also impede purification of recovered monomers and may impact downstream polymerization processes. The impact of these contaminants will be explored in a future study. It is our hope that this work will be utilized as a formulation guide by polymer producers and compounds, and will ignite increasing foresight for down-stream separation management in mixed polyester depolymerization as the field progresses.

CRediT authorship contribution statement

Ryan W. Clarke: Writing – review & editing, Writing – original draft, Methodology, Formal analysis, Data curation, Conceptualization. **Briona J. Carswell:** Writing – original draft, Formal analysis, Data curation. **Jason S. DesVeaux:** Writing – review & editing, Writing – original draft, Formal analysis. **Levi J. Hamernik:** Writing – review & editing, Investigation, Data curation. **Clarissa Lincoln:** Writing – review & editing, Formal analysis, Data curation. **Vinod K. Konaganti:** Writing – review & editing, Visualization, Funding acquisition, Conceptualization. **Rufina G. Alamo:** Writing – review & editing, Writing – original draft, Investigation, Formal analysis, Data curation. **Katrina M. Knauer:** Writing – review & editing, Writing – original draft, Resources, Project administration, Methodology, Investigation, Funding acquisition, Formal analysis, Data curation, Conceptualization.

Declaration of competing interest

Katrina M. Knauer is an inventor on WO2025015059A1, a patent on Downstream process for separating a mixture of depolymerized polyester products produced from methanolysis. This patent has been licensed to EsterCycle™. All other authors declare that they have no known competing financial interests or personal relationships that could have appeared to influence the work reported in this paper.

Acknowledgements

This work was authored by the National Renewable Energy Laboratory, operated by Alliance for Sustainable Energy, LLC, for the U.S. Department of Energy (DOE) under Contract No. DE-AC36-08GO28308. Additionally, funding for some components of this work was provided by the U.S. Office of Energy Efficiency and Renewable Energy, Advanced Materials and Manufacturing Technologies Office (AMMTO) and Bioenergy Technologies Office (BETO) as part of the BOTTLE™ Consortium. RGA and BJC acknowledge funding by the National Science Foundation, DMR-2154026.

Supplementary materials

Supplementary material associated with this article can be found, in the online version, at doi:10.1016/j.resconrec.2025.108439.

Data availability

Data will be made available on request.

References

Aguado, A., Becerra, L., Martinez, L., 2023. Glycolysis optimization of different complex PET waste with recovery and reuse of ethylene glycol. Chem. Pap. 77, 3293–3303.
Alizadeh, A., Richardson, L., Xu, J., McCartney, S., Marand, H., Cheung, Y.W., Chum, S., 1999. Influence of structural and topological constraints on the crystalliation and melting behavior of polymers. 1. Ethylene/1-octene copolymers. Macromolecules 32, 6221–6235.
Andini, E., Bhalode, P., Gantert, E., Sadula, S., Vlachos, D.G., 2024. Chemical recycling of mixed textile waste. Sci. Adv. 10, eado6827.
Arifuzzaman, M., Sumpter, B.G., Demchuk, Z., Do, C., Arnould, M.A., Rahman, M.A., Cao, P.-F., Popovs, I., Davis, R.J., Dai, S., Saito, T., 2023. Selective deconstruction of mixed plastics by a tailored organocatalyst. Mater. Horiz. 10, 3360–3368.
Barnard, E., Arias, J.J.R., Thielemans, W., 2021. Chemolytic depolymerization of PET: a review. Green. Chem. 23, 3765–3789.
Biodegradable Plastics Market Global Forecast to 2029, 2024. Res. Mark. Rep.
Cao, F., Wang, L., Zheng, R., Guo, L., Chen, Y., Qian, X., 2022. Research and progress of chemical depolymerization of waste PET and high-value application of its depolymerization products. RSC Adv. 12, 31564–31576.
Cao, J., Liang, H., Yang, J., Zhu, Z., Deng, J., Li, X., Elimelech, M., Lu, X., 2024. Depolymerization mechanisms and closed-loop assessment in polyester waste recycling. Nat. Commun. 15, 6266.
Clark, R.A., Shaver, M.P., 2024. Depolymerization within a circular plastics system. Chem. Rev. Soc. 124, 2617–2650.

Coates, G.W., Getzler, Y.D.Y.L., 2020. Chemical recycling to monomer for an ideal, circular polymer economy. Nat. Rev. Mater. 5, 501–516.
Cranston, E., Kawada, J., Raymond, S., Morin, F.G., Marchessault, R.H., 2003. Cocrystallization model for synthetic biodegradable poly(butylene adipate-co-butylene terephthalate). Biomacromolecules 4, 995–999.
DesVeaux, J.S., Uekert, T., Curley, J.B., Choi, H., Liang, Y., Singh, A., Mante, O.D., Beckham, G.T., Jacobsen, A.J., Knauer, K.M., 2024. Mixed polyester recycling can enable a circular plastic economy with environmental benefits. One Earth 7, 2204–2222.
Gana, Z., Kuwabaraa, K., Yamamotob, M., Abea, H., Doi, Y., 2003. Solid-State structures and thermal properties of aliphatic—Aromatic poly(butylene adipate-co-butylene terephthalate) copolyesters. Polym. Degrad. Stab. 83, 289–300.
Hong, M., Chen, E.Y.-X., 2017. Chemically recyclable polymers: a circular economy approach to sustainability. Green. Chem. 19, 3692–3706.
Jie, H., Ke, H., Wenjie, Q., Zibin, Z., 2006. Process analyis of depolymerization polybutylene terephthalate in supercritical methanol. Polym. Degrad. Stab. 91, 2527–2531.
Li, Y., Wang, S., Qian, S., Liu, Z., Weng, Y., Zhang, Y., 2024. Depolymerization and re/upcycling of biodegradable PLA plastics. ACS Omega 9, 13509–13521.
Loyer, C., Regnier, G., Duval, V., Richaud, E., 2021. Multiscale study of poly(Butylene Terephthalate) hydrolysis. Polym. Degrad. Stab. 192, 109690.
Mencik, Z.J., 1975. The crystal structure of poly(tetramethylene terephthalate). Polym. Sci. Polym. Phys. Ed. 13, 2173–2181.
Minke, R., Blackwell, J., 1979. Polymorphic structure of poly(tetramethylene adipate). J. Macromol. Sci. Phys. 3, 407–417.
Nicholson, S.R., Rorrer, N.A., Carpenter, A.C., Beckham, G.T., 2021. Manufacturing energy and greenhouse gas emissions associated with plastics consumption. Joule 5, 673–686.
Nixon, K.D., Schyns, Z.O.G., Luo, Y., Ierapetritou, M.G., Vlachos, D.G., Korley, L.T.J., Epps III, T.H., 2024. Analyses of circular solutions for advanced plastics waste recycling. Nat. Chem. Eng. 1, 615–626.
Pang, W., Li, B., Wu, Y., Zeng, Q., Yang, J., Zhang, Y., Tian, S., 2024. Upgraded recycling of biodegradable PBAT plastic: efficient hydrolysis and electrocatalytic conversion. Chem. Eng. J. 486, 150342.
Sardon, H., Jehanno, C., Demarteau, J., Mantoine, D., Arno, C., Ruiperez, F., Hedrick, J., Dove, A., 2021. Selective chemical upcycling of mixed plastics guided by a thermally stable organocatalyst. Angew. Chem. Int. Ed. 60, 6710–6717.
Schwab, S.T., Baur, M., Nelson, T.F., Mecking, S., 2024. Synthesis and deconstruction of polyethylene-type materials. Chem. Rev. 5, 2327–2351.
Shen, C., Zhao, X., Long, Y., An, W., Zhou, X., Liu, X., Xu, S., Wang, Y.-Z., 2023. Approach for the low carbon footprint of biodegradable plastic PBAT: complete recovery of its every monomer via high-efficiency hydrolysis and separation. ACS Sus. Chem. Eng. 11, 2005–2013.
Shi, C., Quinn, E.C., Diment, W.T., Chen, E.Y.-X., 2024. Recyclable and (Bio)degradable polyesters in a circular plastics economy. Chem. Rev. Soc. 124, 4393–4478.
Spicer, A.J., Brandolese, A., Dove, A.P., 2024. Selective and sequential catalytic chemical depolymerization and upcycling of mixed plastics. ACS Macro Lett. 13, 189–194.
Vidal, F., van der Marel, E.R., Kerr, R.W.F., McElroy, C., Schroeder, N., Mitchel, C., Rosetto, G., Chen, T.T.D., Bailey, R.M., Hepburn, C., Redgwell, C., Williams, C.K., 2024. Designing a circular carbon and plastics economy for a sustainable future. Nature 626, 45–57.
Weng, Y., Hong, C.-B., Zhang, Y., Liu, H., 2023. Catalytic depolymerization of polyester plastic toward closed-loop recycling and upcycling. Green. Chem. 26, 571–592.
Xu, G., Wang, Q., 2022. Chemically recyclable polymer materials: polymerization and depolymerization cycles. Green. Chem. 6, 2321–2346.
Yang, R., Xu, G., Dong, B., Guo, X., Wang, Q., 2022. Selective, sequential, and “one-pot” depolymerization strategies for chemical recycling of commercial plastics and mixed plastics. ACS Sus. Chem. Eng. 10, 9860–9871.
Yang, R., Xu, G., Lv, C., Dong, B., Zhou, L., Wang, Q., 2020. Zn(HDMS) as a versatile transesterification catalyst for polyesters synthesis and degradation toward a circular materials economy approach. ACS Sus. Chem. Eng. 8, 18347–18353.
Zheng, W.-Z., Li, X., Xie, J., Zhang, Z.-Y., Wang, P.-L., Huang, D., Ren, Z.-L., Ji, J.-H., Wang, G.-X., 2024. Closed-loop recycling of biodegradable poly(butylene adipate-co-terephthalate) based on hydrolysis and repolymerization strategy. J. Env. Chem. Eng. 12, 114354.